ELSEVIER

Biophysical Chemistry 109 (2004) 361–373

Biophysical Chemistry

www.elsevier.com/locate/bpc

# Influence of local anesthetics on the phosphatidylcholine model membrane: small-angle synchrotron X-ray diffraction and neutron scattering study☆

Daniela Uhríková[a], Gert Rapp[b], Sergej Yaradaikin[c], Valentin Gordeliy[c,d,e], Pavol Balgavý[a,*]

[a]*Laboratory of Biophysics, Department of Physical Chemistry of Drugs, Faculty of Pharmacy, Comenius University, Odbojárov 10, 832 32 Bratislava, Slovakia*

[b]*Max Planck Institute for Colloid and Interface Science Golm-Potsdam, c/o HASYLAB, DESY, Hamburg, Germany*

[c]*Frank's Laboratory of Neutron Physics, Joint Institute for Nuclear Research, Dubna, Russia*

[d]*Biologische Strukturforschung IBI-2, Forschungszentrum Jülich, Jülich, Germany*

[e]*Center for Biophysics and Physical Chemistry of Supramolecular Structures, Faculty of Molecular and Biological Physics, Moscow Institute for Physics and Technology, Dolgoprudny, Russia*

Received 6 October 2003; received in revised form 18 December 2003; accepted 19 December 2003

**Abstract**

The phase preferences of egg yolk phosphatidylcholine (EYPC) have been examined in the presence of tertiary amine anesthetics [2-(propyloxy)phenyl]-2-(1-piperidinyl)ethyl ester of carbamic acid (C3A) and [2-(heptyloxy)phenyl]-2-(1-piperidinyl)ethyl ester of carbamic acid (C7A, heptacaine). Using the synchrotron small-angle X-ray diffraction (SAXD), it is shown that the C3A anesthetic induces the cubic and hexagonal ($H_I$) phases at $2 \geq$ C3A:EYPC $> 0.5$ and $H_2O$:EYPC $\leq 40$ molar ratios. In contrast, longer alkyloxy chain homolog C7A has no effect on the bilayer arrangement of EYPC at C7A:EYPC $\leq 1$ molar ratios as observed by SAXD in C7A + EYPC mixtures hydrated at $H_2O$:EYPC $\leq 40$ molar ratios, as well as in sonicated C7A + EYPC mixtures hydrated in excess water as proved by the small-angle neutron scattering (SANS). The bilayer thickness $d_L$ decreases and the bilayer C7A surface area $S_{C7A}$ increases with the increase of C7A:EYPC molar ratio. It is suggested that the ability of tertiary amine local anesthetics to influence the $d_L$ and $S_{C7A}$ values and EYPC polymorphism is caused by their effective molecular shape and by charge. The possibility that anesthetic molecules may exert some of their biological effects by virtue of these properties is discussed.


*Keywords:* Lipid bilayer; Local anesthetic; [2-(alkyloxy)phenyl]-2-(1-piperidinyl)ethyl esters of carbamic acid; Phosphatidylcholine; X-Ray diffraction; Neutron scattering

☆ Dedicated to Prof. Dr Jozef Čižmárik on the occasion of his birthday.

*Corresponding author. Tel.: +421-2-50259-276; fax: +421-2-55572-065.
*E-mail address:* pavol.balgavy@fpharm.uniba.sk (P. Balgavý).

0301-4622/04/$ - see front matter © 2003 Elsevier B.V. All rights reserved.
doi:10.1016/j.bpc.2003.12.010

## 1. Introduction

Tertiary amine local anesthetics like other amphiphiles intercalate into the bilayer between phospholipid molecules in membranes, their polar parts interact with phospholipid polar fragments and their lipophilic parts insert in the bilayer hydrophobic region. Molar ratios of amphiphile:phospholipid and phospholipid:water, and geometrical parameters of interacting molecules such as the molecular volume, the molecular surface area at the aqueous phase – bilayer interface and the hydrocarbon substituent chain lengths determine structural properties of the bilayer [1–3]. At high concentrations, the interaction of anesthetic molecules with phospholipid bilayer can cause its destabilization and induction of non-bilayer phases [4–7]. In the present work, the effect of tertiary amine local anesthetic [2-(alkyloxy)phenyl]-2-(1-piperidinyl)ethyl esters of carbamic acid (CnA, $n=3$ or 7 is the number of carbon atoms in the alkyloxy substituent) on the structure of egg yolk phosphatidylcholine (EYPC) model membranes, and the polymorphic phase preferences of C7A+EYPC mixtures are studied using small-angle X-ray diffraction (SAXD) and neutron scattering (SANS). Heptacaine (C7A) is one of the most potent local anesthetics – its relative surface anesthesia potency is approximately 100 times higher in comparison to the standard cocaine, while the relative surface anesthesia potency of clinically used dibucaine is only 10 times higher [8]. Comparing to procaine, its relative efficiency to block the action potential on axons and nerves is 94 and 98 times higher, respectively, while the widely studied and clinically used lidocaine is only 7.1 and 3.4 times more efficient than procaine [8,9]. Besides local anesthetic potencies, heptacaine and its homologs are efficient antimicrobials [10] and antiphotosynthetic agents [11]. It is possible that some of their biological effects could be caused by their ability to affect the bilayer structure and to induce non-bilayer structures in membranes.

## 2. Materials and methods

### 2.1. Chemicals

CnA anesthetics were prepared as described in Ref. [12]. EYPC was isolated from fresh egg yolks and purified by a column chromatography as described in Ref. [13]. Its molar weight $M_{EYPC}=$ 779.7 g/mol was calculated from its acyl chain composition as in Ref. [14]. Its purity was controlled by the two-dimensional thin-layer chromatography and by the spectrophotometric determination of conjugated dienes as indicators of lipid oxidation [15]. Heavy water (99.98% $^2H_2O$) was obtained from Izotop (Moscow, Russia). The organic solvents used for EYPC preparation, purification and chromatographic analysis as well as for sample preparation were obtained from Mikrochem (Bratislava, Slovakia). The other chemicals were purchased from Lachema (Brno, Czech Republic). For UV–VIS spectrophotometry, organic solvents of spectral purity were used; the other commercial chemicals were of analytical purity. The water and organic solvents except of those of spectral purity and heavy water were redistilled before use. The Silufol chromatographic plates were from Kavalier (Sázava, Czech Republic).

### 2.2. Sample preparation for SANS

C7A+EYPC were mixed in chloroform–methanol (1:1 v/v) in a glass tube. Organic solvents were evaporated under nitrogen gas and evacuated in the presence of $P_2O_5$ for several hours at room temperature. Heavy water was added to obtain the final EYPC concentration of 10 mg/ml. The tube with this mixture was purged with pure gaseous nitrogen and sealed. Its content was dispersed by hand shaking and sonication in the UC 405 BJ-1 bath sonicator (Tesla, Vráble, Slovakia) at room temperature. After that, the aqueous C7A+EYPC dispersions were sonicated for 50 min at 5 °C under gaseous nitrogen in 2-min intervals using the UZ-DEZ 20 kHz titanium probe-type sonicator (Chirana, Piešťany, Slovakia). After sonication, the dispersions were centrifuged for 20 min on the high-speed laboratory centrifuge type 310 (Mechanika Precyzyjna, Warsaw, Poland) in order to remove particles released from the titanium probe at the sonication. The pH value of the samples was in the range 5.0–5.5. Under these conditions, the concentration of conjugated dienes, estimated spectrophotometrically according to Ref.

[15] as a measure of the EYPC peroxidation, does not increase during the sample preparation. There were also no indications of EYPC decomposition as checked by a two-dimensional thin layer chromatography. Finally, the samples were poured into quartz cells (Hellma, Müllheim, Germany) to provide the 2 mm sample thickness.

### 2.3. Sample preparation for SAXD

CnA + EYPC were mixed in chloroform–methanol, and the organic solvents were removed as described above. Redistilled water at a molar ratio $H_2O$:EYPC = $m$ was then added. The $H_2O$ + EYPC + CnA mixtures were homogenized in flame-sealed glass tubes by several cycles of forth and back centrifugation. The tubes were opened and the homogenized mixtures were placed between 25-μm thick mica windows in the 5-mm hole in the center of 0.8 mm steel plates (sandwich samples). The mica windows were glued to the steel plates by a high vacuum silicon grease (Wacker, Munich, Germany) to prevent the evaporation of water.

### 2.4. Small-angle neutron scattering

The SANS measurements were performed at the small-angle time-of-flight axially symmetric neutron scattering spectrometer MURN (named now YuMO in honor of deceased Yu.M. Ostanevich) at the IBR-2 fast pulsed reactor of the Frank's Laboratory of Neutron Physics, Joint Institute for Nuclear Research in Dubna [16,17]. The sample temperature was set and controlled electronically at 20 ± 0.1 °C. The sample was equilibrated for 1 h at this temperature before measurement. The SANS patterns were measured in the range of scattering vector values $Q = 4\pi\sin\theta/\lambda = 0.007$–$0.13$ Å$^{-1}$ where $2\theta$ is the scattering angle and $\lambda$ the wavelength of neutrons. The scattering patterns were corrected for background effects. The coherent scattering cross section was obtained by using a vanadium standard scatterer.

### 2.5. Small-angle X-ray diffraction

The diffraction data for EYPC + CnA samples were obtained using the X13 double focusing monochromator-mirror camera of the European Molecular Biology Laboratory Outstation at the Deutsches Elektronen Synchrotron (DESY) in Hamburg on the storage ring DORIS (see Ref. [18] and references therein). At this beam line, the wavelength selected by a Ge(111) crystal is $\lambda$ = 0.15 nm. The reciprocal spacing $s = 2\sin\theta/\lambda$, where $2\theta$ is the scattering angle, was calibrated using the rat-tail tendon and silver behenate as standards [19,20]. The diffraction data were analyzed using the evaluation program OTOKO [21]. Before measurements, the samples were equilibrated at room temperature for several hours in a dark place. During measurements, the sample was held in a thermostatically controlled sample holder at 20 ± 0.1 °C. In selected experiments, the sample was heated at 1 K/min rate.

## 3. Results and discussion

### 3.1. Phospholipid polymorphism

The SAXD is the preferred method for identification of phospholipid polymorphism. The long range ordering of lipid aggregates onto one-, two-, or three-dimensional lattices gives rise to Bragg diffraction peaks whose reciprocal spacings are in characteristic ratios, e.g. $s_h = h/d$ (lamellar phase $L$), $s_{hk} = 2(h^2 + k^2 + hk)^{0.5}/3^{0.5}a$ (hexagonal phase $H$) or $s_{hkl} = (h^2 + k^2 + l^2)^{0.5}/a$ (cubic phase $C$), where $h$, $k$, $l = 0$, 1, 2, 3... are the Miller indices, and $d$ and $a$ are the unit cells parameters [22,23]. It is well known that hydrated EYPC forms the one-dimensional fluid $L_a$ phase with stacked bilayers separated by layers of water over broad temperature and hydration ranges [22,24]. We have confirmed this finding in the range of $m$ = 16–40 molar ratios (Table 1).

In the C3A + EYPC mixtures, we have observed the SAXD pattern characteristic of the $L$ phase up to C3A:EYPC = 0.5:1 and $m$ = 30 molar ratios (not shown). At higher C3A:EYPC molar ratios, the SAXD patterns consisted of superposition of diffraction peaks of different phases. For example, in the C3A + EYPC mixture at molar ratio C3A:EYPC = 2:1 and low hydration ($m$ = 16), four equidistant reflections of lamellar phase $L$ with the repeat period $d$ = 4.69 nm and three reflections

marked *X* at *s* spacings 0.803 $nm^{-1}$, 1.012 $nm^{-1}$ and 1.227 $nm^{-1}$ are seen (Fig. 1a). Since a minimum of four reflections are needed to identify the symmetry aspect of the mesophase [25], the identification of phase *X* would need a further more detailed study. With the increasing amount of water ($m=30$) a new phase appeared. Except of lamellar and *X* phases, the SAXD pattern has indicated a hexagonal phase *H* with reflections spaced in the $s^2$ ratio of 1:3:4:7:9. When the content of C3A was decreased, the *X* phase disappeared. At the molar ratios of C3A:EYPC = 1:1 and $m=16$, only one weak reflection of the *X* phase was observed besides the peaks of the *L* phase. The samples at molar ratios of C3A:EYPC = 1:1 and $m=30$ have shown the presence of two phases: lamellar *L* and hexagonal *H* (Fig. 1b). The summary of phase behavior in dependence on the molar ratio of C3A:EYPC at selected hydrations *m* is given in Table 1. Using the same samples, we have observed lamellar-type, hexagonal-type and isotropic proton-decoupled $^{31}$P-NMR signals in samples where the *L*, *H* and *X* phases were found by SAXD (Uhríková and Balgavý, unpublished). The samples containing the *X* phase were very viscous. These data indicate, that the *X* phase could be cubic.

We have studied the temperature dependence of diffraction patterns with reflections of *L* and *H* phases. With the increasing temperature, the amount of the *H* phase decreased and that of the *L* phase increased, as shown on the temperature dependence of integral intensities of first diffraction maxima of both phases in the C3A:EYPC = 1:1 (mol/mol) and $H_2O$:EYPC = 30:1 (mol/mol) mixture (Fig. 2).

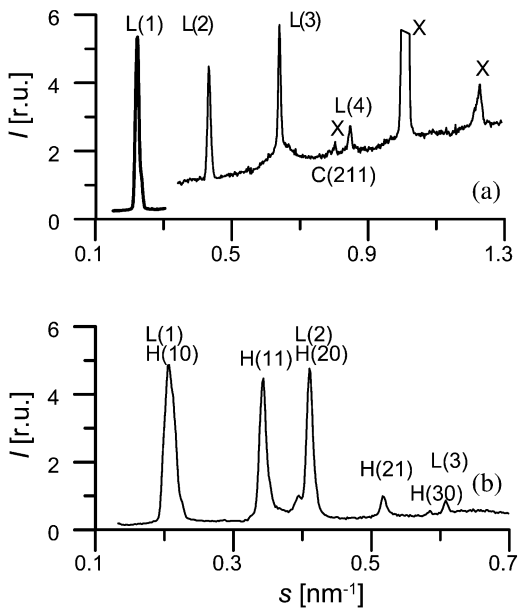


Fig. 1. SAXD patterns of C3A:EYPC = 2:1 (mol/mol) and $H_2O$:EYPC = 16:1 (mol/mol) mixture (a) and of C3A:EYPC = 1:1 (mol/mol) and $H_2O$:EYPC = 40:1 (mol/mol) mixture (b). In panel (a), the *L*(1) peak is attenuated and *X* peak at 1.012 $nm^{-1}$ is truncated.

The lipid polymorphic phase preferences can be explained using the concept of an effective lipid molecular shape. Cone-shaped molecules form normal spherical or cylindrical micelles, cylinder-shaped molecules form bilayers and vesicles, and inverted cone-shaped molecules inverted spherical or cylindrical micelles; the micelles can aggregate into ordered phases [26]. As a rule, inverted hexagonal $H_{II}$ phases transform into lamellar phases when the temperature is decreased [27–29] –

Table 1
Polymorphic phase behaviour of the C3A + EYPC and C7A + EYPC mixtures

| $H_2O$:EYPC (mol:mol) | C3A:EYPC (mol:mol) | | | | C7A:EYPC (mol:mol) | |
|---|---|---|---|---|---|---|
| | 2:1 | 1.5:1 | 1:1 | 0.5:1 | 1:1 | 0:1 |
| 16:1 | *L*+*X* | *L*+*X* | *L*+*X** | *L* | *L* | *L* |
| 20:1 | ** | ** | ** | ** | *L* | *L* |
| 30:1 | *L*+*X*+*H* | *L*+*X*+*H* | *L*+*H* | *L* | *L* | *L* |
| 40:1 | *L*+*X*+*H* | ** | *L*+*H* | ** | *L* | *L* |

*Only one weak reflection of *X* phase was observed at 1.01 $nm^{-1}$; **Not measured.

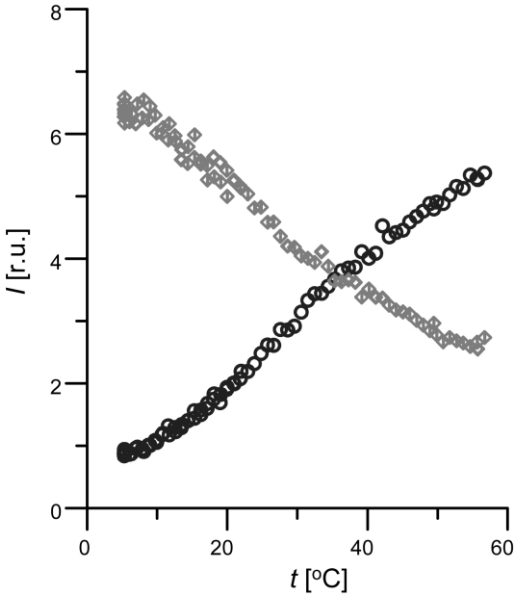


Fig. 2. The temperature dependence of integral intensity $I$ (in relative units) of the $L(1)$ and $H(10)$ reflections in C3A:EYPC (1:1 mol/mol) and $H_2O$:EYPC = 30:1 (mol/mol) mixture. Circles: $L(1)$, diamonds: $H(10)$.

the number of gauche conformers in the lipid hydrocarbon chains decreases, the chain length increases and the effective molecular shape converts from the inverted cone to cylinder. The C3A anesthetic is known to form normal micelles in the aqueous phase [30,31], its effective molecular shape can be described as a cone. Extending the concept of effective shape to mixed lipid + amphile systems [32,33], the C3A + EYPC system can be described as a cone-shaped or cylindrical depending on the C3A:EYPC molar ratio and temperature. The conversion of the $H$ phase into the $L$ phase with the increase of temperature seen in Fig. 2 is an evidence that the $H$ phase is of the normal $H_I$ type.

In contrast to C3A + EYPC mixtures, no diffraction peaks characteristic of non-lamellar phases were observed in the C7A + EYPC mixtures at C7A:EYPC = 1:1 and up to $H_2O$:EYPC = 40:1 molar ratios (Table 1). We have confirmed our earlier finding obtained with a conventional X-ray source that C7A + EYPC forms the lamellar $L_a$ phase in the molar ratio ranges studied [34]. Since the formation of non-lamellar phases is sensitive to the hydration $m$ (see Table 1), we have studied the C7A + EYPC mixtures also at high excess of the aqueous phase. The SAXD patterns of these samples consisted of a weak continuous scattering without sharp diffraction peaks. The p$K_a$ value of C7A in the aqueous phase is 8.9 [35], the p$K_a$ in the EYPC lipid phase is decreased to 7.6 [36]. The samples with an excess of aqueous phase were prepared at pH 5.0–5.5, the CnA molecules are therefore intercalated between EYPC molecules as cations. When the surface of bilayers dispersed in the aqueous phase becomes positively charged by insertion of cationic amphiphiles and the charge density exceeds 1–2 $\mu C/cm^2$, unilamellar vesicles form spontaneously from multilamellar structures [37]. Since the C7A anesthetic forms micelles in the aqueous phase [30,31], mixed micelles could form in excess aqueous phase too. Recently, Hata et al. [7] have observed formation of such mixed micelles in the tertiary amine anesthetic + dipalmitoylphosphatidylcholine (DPPC) mixtures with a broad anesthetic concentration range where bilayer vesicles and mixed micelles coexisted. Consequently, the continuous scattering observed with C7A + EYPC aggregates in excess aqueous phase could be caused by unilamellar vesicles as well as by mixed micelles.

We have tested the possibility of micelle formation in C7A + EYPC mixtures by using SANS. Before the measurements, the samples were ultrasonicated to convert multilamellar vesicles (if any) into unilamellar ones in order to simplify the interpretation of scattering patterns. As an example, the scattering pattern of sample prepared at C7A:EYPC = 1:1 molar ratio is shown in Fig. 3. In this pattern as well as in the other SANS patterns obtained in the present study, the absence of the pronounced first order Bragg diffraction peak is notable. This peak was observed in SANS experiments with multilamellar vesicles [38] and with a mixture of unilamellar and multilamellar vesicles prepared by sonication [39]. The absence of this peak is evidence that the samples did not contain an appreciable amount of multilamellar vesicles.

The coherent scattering intensity $I(Q)$ per unit neutron flux on the sample and per unit volume

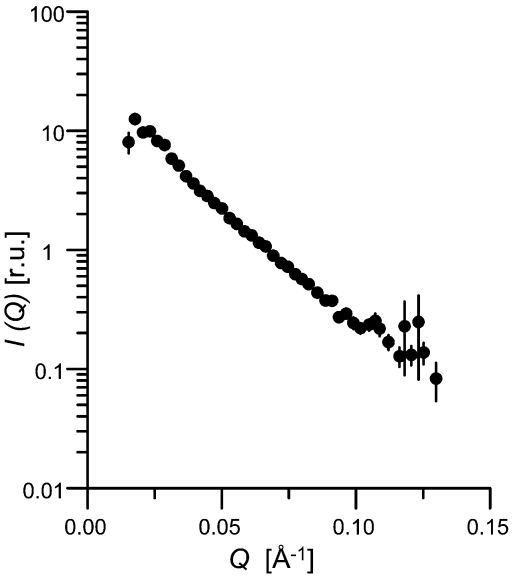


Fig. 3. The dependence of SANS scattering intensity $I(Q)$ on the scattering vector value $Q$ for sonicated C7A:EYPC (1:1 mol/mol) mixture in heavy water. The plotted points indicate the mean values obtained by averaging over the seven circular detectors of YuMO and the error bars the S.E. of the mean value.

of the sample can be written for small scattering angles as

$$I(Q) = I(0)\exp(-Q^2R_g^2/r)Q^{r-3}, \quad (1)$$

where $I(0)$ is the constant dependent on concentration, volume and scattering properties of the objects, $R_g$ is the radius of gyration of the scattering object and $r=1$, 2 and 3 holds for infinite sheet-like objects (like planar lipid bilayers), for rod-like objects of infinite length and uniform cross section (like cylindric micelles), and for globular objects (like spheroid micelles), respectively (see Refs. [40–42]). This approximation is valid also for finite size objects when $L^{-1} \leq Q \leq R_g^{-1}$, where $L$ is the longest size of the object. The value $r=1$ is a good approximation also for polydisperse hollow spheres such as unilamellar vesicles [43–46]. Using the Kratky–Porod plots of $\ln[I(Q)Q^r]$ vs. $Q^2$, it is possible to discriminate between different geometrical forms of C7A+EYPC aggregates. The Kratky–Porod plots of SANS data are shown in Fig. 4. We have fitted these data in the region of 0.005 $Å^{-2} \leq Q^{-2} \leq 0.01$ $Å^{-2}$ and extrapolated the fit down to 0.0005 $Å^{-2}$. It is seen that the data are best fitted supposing $r=1$, the experimental points deviate upwards from the extrapolated curves when supposing $r=2$ and $r=3$. We can conclude that at the C7A:EYPC=1:1 molar ratio in the sample and in the excess of aqueous phase, the mixed spheroid or cylindric micelles does not form in a significant amount to be detected by SANS. We have obtained the same result at lower C7A:EYPC molar ratios. Since the SANS as used in the present paper cannot discriminate between the sheet-like objects and polydisperse hollow spheres, we cannot exclude a possibility that the vesicles disaggregated into sheet-like objects, e.g. into discoid mixed micelles with relatively large lateral dimensions (bilayer micelles—'bicelles'). Nevertheless, we can conclude that a relatively small change in the CnA molecular structure—the increase of alkyloxy substituent chain length from three to seven carbons—changes the effective molecular shape of mixed CnA+EYPC system from the cone to cylinder at CnA:EYPC=1:1 molar ratio.

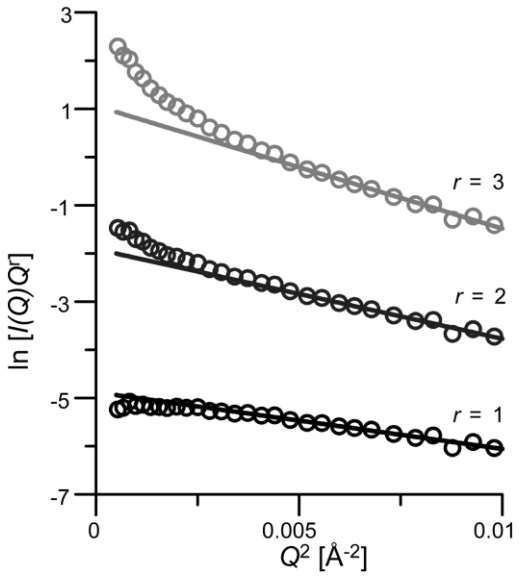


Fig. 4. The Kratky-Porod plots of SANS data for sonicated C7A:EYPC (1:1 mol/mol) mixture in $^2H_2O$.

### 3.2. Bilayer thickness and lipid surface area

The SANS and SAXD data provide information on the bilayer geometrical parameters – lipid bilayer thickness and surface area $S$ per one lipid molecule at the bilayer–aqueous phase interface. It is well known that the bilayer thickness parameter $d_g$ can be calculated from the radius of gyration $R_g$ measured with vesicles dispersed in $^2H_2O$ (see Refs. [39,41,43] and references therein) as:

$$d_g \approx 12^{0.5} R_g \quad (2)$$

The thickness parameter $d_g$ can be used as a measure of the phosphatidylcholine bilayer thickness in unilamellar vesicles—the value of $d_g$ is a linear function of the transbilayer distance between the lipid phosphate groups in the opposing monolayers [45,46]. Since the Kratky–Porod plot of SANS data of the control sample (C7A:EYPC = 0:1) displayed a pronounced oscillation at $Q^2 \leq 0.005$ Å$^{-2}$ due to small vesicle radius and its polydispersity in the sonicated sample (For example, see Figs. 2, 4, 6, and 7 in Ref. [44]), the control value of $d_g$ was calculated from the SANS data obtained with extruded (mean diameter 500 Å) unilamellar EYPC vesicles and published in Ref. [44]. The values of $d_g$ were evaluated from the SANS data in the region 0.001 Å$^{-2} \leq Q^2 \leq 0.01$ Å$^{-2}$ by using Eqs. (1) and (2) (with $r = 1$). To obtain the values of bilayer thickness from the SAXD data, the C7A:EYPC molar ratio in the bilayer must be known. The C7A:EYPC molar ratio in the sample is higher than that in the bilayer in the volume excess of the aqueous phase because of the partition equilibrium of C7A between the bilayer and the aqueous phase. We have estimated earlier the C7A cation partition coefficient between the lipid bilayer of unilamellar EYPC vesicles and aqueous phase (pH 4.5) at $0.08 \leq$ C7A:EYPC $\leq 0.88$ molar ratios in the bilayer using the C7A cation sensitive electrode [47], so we recalculated the sample C7A:EYPC molar ratio into the bilayer C7A:EYPC = $n$ molar ratio by using these C7A partition coefficient data. The C7A + EYPC 'dry bilayer' thickness is calculated then from the SAXD lamellar repeat period $d$ using the Luzzati's model of separated lipid and water layers [22] as:

$$d_L = d(V_{\mathrm{EYPC}} + nV_{\mathrm{C7A}})/(V_{\mathrm{EYPC}} + nV_{\mathrm{C7A}} + mV_W), \quad (3)$$

where $V_{\mathrm{EYPC}}$, $V_{\mathrm{C7A}}$ and $V_W$ are the molecular volume of EYPC, C7A and water, respectively. The value of $V_{\mathrm{EYPC}} = 1273.9 \pm 0.4$ Å$^3$ used in Eq. (3) was obtained from the partial specific volume $\bar{V}_{20,\mathrm{EYPC}} = 0.9839 \pm 0.0003$ cm$^3$/g measured in EYPC vesicles at 20 °C in Ref. [48], by using the EYPC molar weight $M_{\mathrm{EYPC}} = 779.7$ g/mol. The temperature dependence of the partial specific volume of C7A was measured in the aqueous phase at pH 5 in the range 30.5–41.5 °C (Fig. B in Ref. [49]). Supposing that the thermal volume expansion coefficient is independent of temperature, we have calculated the C7A partial specific volume $\bar{V}_{20,\mathrm{C7A}} = 1.1486 \pm 0.0040$ cm$^3$/g by extrapolation of these data to 20 °C. When located in the fluid DPPC bilayers, the partial specific volume of C7A is only $0.9 \pm 0.4$% less than in the aqueous phase [50]. Supposing the same small reduction of the C7A partial specific volume in the fluid EYPC bilayers, we have obtained the molecular volume of C7A located in the EYPC bilayer $V_{\mathrm{C7A}} = 576.3 \pm 2.3$ Å$^3$. The molecular volume of water at 20 °C is $V_W = 29.97$ Å$^3$ [51]. The Luzzati's model of 'dry bilayer' imposes limits on the values of $m$ used in Eq. (3). At low values of $m$, the water molecules are located in the lamellar phase, but the bilayer polar region is not fully hydrated [52]. At high values of $m$, the bilayers are fully hydrated, but the increased water amount causes the formation of vesicles with curved bilayers. In the vesicular system, the water is located not only in bilayers and between them, but also between vesicles [53]. Therefore, the gravimetric values of $m$ determined in the whole sample and used in Eq. (3) underestimate the value of $d_L$ in the system containing vesicles besides planar bilayers. To overcome these problems, we have estimated the value of $d_L$ as a function of $m$. The value of $d_L$ decreased with the increase of $m$ in the range of $m < 12$ and $m < 18$ in the $n =$

C7A:EYPC = 0 and $n$ = C7A:EYPC = 1.0 sample, respectively. After that, there was a narrow range of $m$ wherein the value of $d_L$ remained constant within the experimental error. Finally, the value of $d_L$ decreased again at $m > 22$ and $m > 29$ in the $n$ = C7A:EYPC = 0 and $n$ = C7A:EYPC = 1.0 sample, respectively. The first decrease of $d_L$ is caused by the hydration of bilayer polar region and, consequently, by the lateral bilayer expansion. The changes in the bilayer hydration with the increasing $m$ are reflected in the EYPC headgroup conformation [52,54,55]. In the absence of C7A, the effective $^{31}$P-NMR chemical shift anisotropy $\Delta\sigma_{\mathrm{eff}}$ in EYPC vesicles decreased for $m < 11$ and then remained constant for $m > 13$; in the $n$ = C7A:EYPC = 1.0 sample, $\Delta\sigma_{\mathrm{eff}}$ decreased up to $m = 22 \pm 3$ and then remained constant up to the highest $m = 104$ studied [52,55]. Combining these results with the SAXD data, one can conclude that the bilayers were fully hydrated at $m > 14$ and $m > 20$ in the $n = 0$ and $n = 1.0$ sample, respectively. The presence of C7A molecules in the bilayer is known to increase the number of anisotropically moving heavy water molecules from $m = 12 \pm 1$ in pure EYPC to $m = 18 \pm 2$ in the $n$ = C7A:EYPC = 1 samples as found by $^2$H-NMR spectroscopy [52], as well as the number of water molecules which are not frozen at 0 °C to $m = 20 \pm 1$ in the $n$ = C7A:DPPC = 1 samples estimated by calorimetry [56]. The increase of the limit of $m$ where the EYPC bilayer hydration occurs to higher value in the presence of C7A is consistent with these data. The second decrease of $d_L$ was most probably an artifact caused by the vesicle formation in the systems studied resulting in the underestimation of $d_L$ as discussed above. Therefore, we have calculated the values of bilayer thickness $d_L$ for $14 \le m \le 20$ and $20 \le m \le 29$ hydrations in the $n$ = C7A:EYPC = 0 and $n$ = C7A:EYPC = 1 samples, respectively.

The averaged values of $d_L$ in the hydration regions discussed above are shown together with the $d_g$ values obtained from SANS data as a function of C7A:EYPC molar ratio in the bilayer $n$ in Fig. 5. From these data, it is seen the $d_g$ and $d_L$ values coincide within experimental error in the control samples ($n = 0$). It is further seen that the bilayer thickness parameter $d_g$ decreases with the

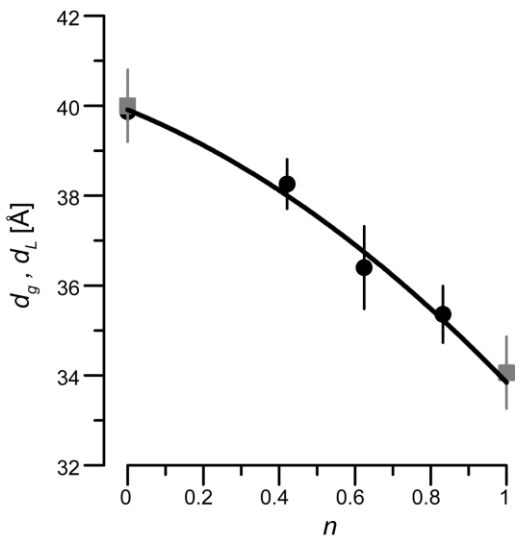


Fig. 5. The dependence of bilayer thickness on the C7A:EYPC molar ratio in the bilayer $n$. Circles – SANS results ($d_g$), squares – SAXD results ($d_L$).

$n$ = C7A:EYPC molar ratio and that the value of $d_L$ obtained from SAXD data at $n = 1$ fits well into this $d_g$ dependence. The cause of the bilayer thickness decrease is simple: the lateral bilayer expansion and the mismatch between the lengths of hydrophobic parts of C7A and EYPC after intercalation of C7A molecules between phospholipids results in the increased population of gauche isomers in lipid hydrocarbon chains in the bilayer hydrophobic center [2] and, consequently, in the thickness decrease.

The SAXD and SANS data can also be used to obtain estimates of the lipid surface area. Using the Luzzati's model of separated lipid and water layers [22], the EYPC surface area $S_{\mathrm{EYPC}}$ in the control sample is given by:

$$S_{\mathrm{EYPC}} = 2V_{\mathrm{EYPC}}/d_i, \qquad (4)$$

where $i = L$ or $g$ and $V_{\mathrm{EYPC}} = 1273.9 \pm 0.4$ Å$^3$ is the molecular volume of EYPC. We have obtained $S_{\mathrm{EYPC}} = 63.90 \pm 0.14$ Å$^2$ from the SANS data and $S_{\mathrm{EYPC}} = 63.5 \pm 1.0$ Å$^2$ from the SAXD data. The surface area $S_{\mathrm{C7A+EYPC}}$ per one EYPC molecule in the mixed C7A + EYPC bilayer can then be obtained from SANS data as:

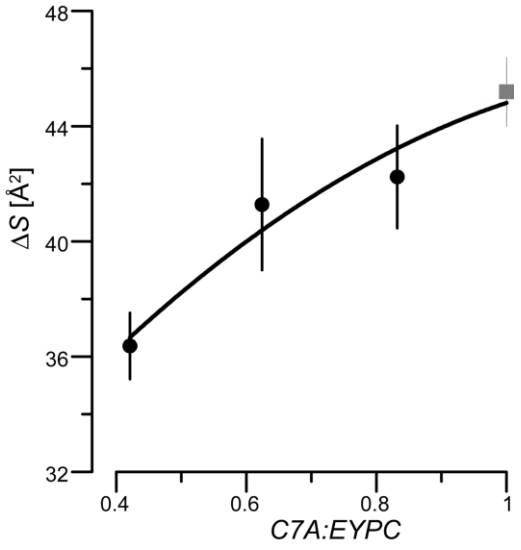


Fig. 6. The dependence of surface area increment $\Delta S$ on the C7A:EYPC molar ratio in the bilayer. Circles – SANS results, square – SAXD result.

$$S_{\mathrm{C7A+EYPC}} = 2(V_{\mathrm{EYPC}} + nV_{\mathrm{C7A}})/d_g, \quad (5)$$

where $n$ is the bilayer C7A:EYPC molar ratio. In case of SAXD data, the value of $S_{\mathrm{C7A+EYPC}}$ can be obtained directly from the repeat period $d$ of the C7A+EYPC lamellar phase as:

$$S_{\mathrm{C7A+EYPC}} = 2(V_{\mathrm{EYPC}} + nV_{\mathrm{C7A}} + mV_W)/d, \quad (6)$$

where $V_W$ is the molecular volume of $H_2O$ and $m$ the $H_2O$:EYPC molar ratio. The change in the bilayer surface area due to intercalation of one C7A molecule at the molar ratio $n$ is given then by:

$$\Delta S = (S_{\mathrm{C7A+EYPC}} - S_{\mathrm{EYPC}})/n. \quad (7)$$

The dependence of $\Delta S$ on the molar ratio $n$ is shown in Fig. 6. It is clearly seen that the value of $\Delta S$ increases with the C7A:EYPC molar ratio in the bilayer, and that the single $\Delta S$ value obtained by SAXD fits well to this dependence. The $\Delta S$ increase can be caused by the electrostatic repulsion of charged C7A molecules located in the bilayer. As far as we know this is the first experimental demonstration that the increment of bilayer surface area due to charged amphiphilic admixture in the bilayer increases with the admixture concentration in the bilayer.

### 3.3. Possible biological consequences

Tertiary amine local anesthetics are cone-shaped molecules and affect the stability of the bilayer. We have found in the present paper, that C3A converts the bilayer into $H_I$ phase at high C3A:EYPC molar ratios and lower temperatures. Tetracaine and dibucaine form mixed micelles with dipalmitoylphosphatidylcholine [7]. Phosphatidylcholines are bilayer-forming lipids, their molecular shape can be described as cylindrical, and the effective molecular shape of anesthetic + phosphatidylcholine mixtures becomes cone-shaped at high anesthetic concentrations. The molecular shape of phosphatidylethanolamines is of inverted cone at higher temperatures and acyl chain unsaturation. Hornby and Cullis [4] have found that the tertiary amine local anesthetics procaine, dibucaine and tetracaine stabilize the bilayer arrangement for egg phosphatidylethanolamine. At neutral pH, the tertiary amine anesthetics are positively charged. Dibucaine was found to induce $H_{II}$ phase in hydrated cardiolipin at neutral pH by charge neutralization [57], decreasing the effective surface area and converting the effective shape of cardiolipin from the cylindrical to inverted cone in anesthetic + cardiolipin mixtures. The positively charged carbisocaine [58] induced the $H_{II}$ phase in negatively charged bilayers formed from total lipids isolated from rat brains (TLRB) at $0.1 <$ carbisocaine:TLRBT $< 0.5$ molar ratios; this $H_{II}$ phase converted to a bilayer phase at carbisocaine:TLRBT $>$ 0.5 molar ratios [6]. Evidently, the tertiary amine local anesthetics display complex effects on the lipid polymorphism depending on both the lipid and anesthetic effective molecular shapes and charges, and on the temperature.

The observed structural changes in model phospholipid membranes can be relevant to mechanisms of biological effects of these compounds. The obvious consequence of non-bilayer structure formation in biological membrane is the disruption of its integrity leading eventually to the cell death.

This mechanism could be responsible for various toxic and biocidal effects of local anesthetics, e.g. for their antimicrobial [10] and antiphotosynthetic [11] activities.

It is well known that the tertiary amine local anesthetics influence the lipid metabolism in cells. For example, the *Acheloplasma laidlawii* cells decreased the molar ratio between the major membrane glucolipids, monoglucosyldiacylglycerol and diglucosyldiacylglycerol, in response of positively charged tetracaine at lipid:tetracaine = 12–15 molar ratios [58]. In rat liver slices, procaine and cinchocaine redirected the metabolism from the synthesis of neutral phospholipids to the accumulation of the negatively charged phospholipids [59]. In synaptosomes, heptacaine and carbisocaine decreased the $^{32}P$ incorporation into neutral phospholipids and increased its incorporation into phosphatidylserine; their effect occurred at concentrations lower by several orders of magnitude as compared to the other local anesthetics studied (procaine, lidocaine, cinchocaine) [60]. This difference could be caused by the substantially higher lipid to aqueous phase partition coefficients of carbisocaine and heptacaine, i.e. by their higher bilayer concentrations comparing to the other anesthetics. These data indicate that cells are able to regulate their lipid composition in order to maintain optimal bilayer composition compensating the anesthetic-induced destabilization of bilayers in their membranes. However, this regulation should differ for different anesthetics not only because of different anesthetics partition coefficients but also because of their effective molecular shapes.

Many biochemical effects of local anesthetics are expressed in $Ca^{2+}$-dependent processes. These effects can be caused by the anesthetic-induced modulation of activities of $Ca^{2+}$-transporting proteins. For example, dibucaine, tetracaine, lidocaine and procaine inhibit the $(Ca^{2+}–Mg^{2+})$-ATPase of synaptosomes [61,62], and dibucaine, tetracaine and heptacaine homolog the $(Ca^{2+}–Mg^{2+})$-ATPase from skeletal muscle sarcoplasmic reticulum [63,64]. The local anesthetics, procaine, lidocaine, tetracaine and dibucaine decrease the denaturation temperature $T_m$ of the sarcoplasmatic reticulum $(Ca^{2+}–Mg^{2+})$-ATPase [63,65]; the decrease of $T_m$ by each anesthetic is proportional to the lipid to water partition coefficient [65]. It has been suggested that besides the direct interaction with the protein, the local anesthetics influence the ATPase activity by disruption of the lipid annulus around the protein [62]. The $(Ca^{2+}–Mg^{2+})$-ATPase is sensitive to changes in the lipid acyl chain length (i.e. in the bilayer thickness) and to the charge of lipid molecules in the lipid annulus surrounding the protein [66]. The effects of anesthetics on ATPase could be caused directly by their charge when located in the lipid annulus as well as indirectly by their effects on the bilayer thickness surrounding the protein.

## Acknowledgments

We thank Prof. J. Čižmárik for the kind gift of local anesthetics and for his continuing interest in our work. This study was supported by the Slovak Ministry of Education grant 1/0123/03 to P.B. Synchrotron beam time was provided under the European Community – Access to Research Infrastructures Action of the Improving Human Potential Programme, contract HPRI-CT-1999-0040/2001-00140, project II-02-016. Neutron beam time was provided under the JINR project 07-4-1031-99/03. P.B. and D.U. thank the staff of FLNP JINR in Dubna and of EMBL Outstation in Hamburg for hospitality. V.G. thanks G. Büldt for the support of this work.

## References

[1] P. Balgavý, F. Devínsky, Cut-off effects in biological activities of surfactants, Adv. Colloid Interface Sci. 66 (1996) 23–63.

[2] J. Gallová, F. Andriamainty, D. Uhríková, P. Balgavý, Interaction of local anesthetic heptacaine homologs with phosphatidylcholine bilayers: spin label ESR study, Biochim. Biophys. Acta 1325 (1997) 189–196.

[3] D. Uhríková, P. Balgavý, G. Rapp, Lipid bilayer thickness and surface area in lamellar phases of hydrated mixtures of dipalmitoylphosphatidylcholine and homologs of local anesthetic heptacaine, Mol. Cryst. Liq. Cryst. 373 (2002) 201–211.

[4] A.P. Hornby, P.R. Cullis, Influence of local and neutral anaesthetics on the polymorphic phase preferences of egg yolk phosphatidylethanolamine, Biochim. Biophys. Acta 647 (1981) 285–292.

[5] K. Ondriaš, A. Staško, P. Balgavý, Spin label study of the perturbation effect of the local anaesthetics tetracaine and dibucaine on synaptosomes at pharmacological concentrations, Biochem. Pharmacol. 36 (1987) 3999–4005.
[6] P. Balgavý, D. Uhríková, K. Ondriaš, Effect of local anesthetic and β-blocker carbisocaine on phospholipid polymorphism, Biológia (Bratislava) 49 (1994) 863–869.
[7] T. Hata, H. Matsuki, S. Kaneshina, Effect of local anesthetics on the bilayer membrane of dipalmitoylphosphatidylcholine: interdigitation of lipid bilayer and vesicle–micelle transition, Biophys. Chem. 87 (2000) 25–36.
[8] V. Račanský, E. Béderová, P. Balgavý, Decrease of gel–liquid crystal transition temperature in dipalmitoyl phosphatidylcholine model membrane in the presence of local anesthetics, Stud. Biophys. 103 (1984) 231–241.
[9] K. Ondriaš, P. Balgavý, S. Štolc, L.I. Horváth, A spin label study of the perturbation effect of tertiary amine anesthetics on brain lipid liposomes and synaptosomes, Biochim. Biophys. Acta 732 (1983) 627–635.
[10] D. Mlynarčík, J. Bittererová, J. Čižmárik, L. Masárová, The effect of piperidinoethylesters of *n*-alkoxyphenylcarbamic acids on bacterial cells, Ceskoslov. Farm. 40 (1991) 25–28.
[11] K. Králová, F. Šeršeň, J. Čižmárik, Inhibitory effect of piperidinoethylesters of alkoxyphenylcarbamic acids on photosynthesis, Gen. Physiol. Biophys. 11 (1992) 261–267.
[12] J. Čižmárik, A. Borovanský, Synthesis, u. v. and i. r. spectra of 2-piperidinoethyl esters of alkoxyphenylcarbamic acids, Chem. Zvesti 29 (1975) 119–123.
[13] W.S. Singleton, M.S. Gray, M.L. Brown, J.L. White, Chromatographically homogenous lecithin from egg phospholipids, J. Am. Oil Chem. Soc. 42 (1965) 53–56.
[14] J. Filípek, K. Gelienová, P. Kovács, P. Balgavý, Effect of lipid autoperoxidation on the activity of the sarcoplasmic reticulum ($Ca^{2+}$–$Mg^{2+}$)-ATPase reconstituted into egg yolk phosphatidylcholine bilayers, Gen. Physiol. Biophys. 12 (1993) 55–68.
[15] R.A. Klein, The detection of oxidation in liposome preparations, Biochim. Biophys. Acta 210 (1970) 486–489.
[16] V.A. Vagov, A.B. Kunchenko, Yu.M. Ostanevich, I.M. Salamatin, Time-of-flight small-angle neutron scattering spectrometer at pulsed reactor IBR-2, JINR Communication P14-83-898 (1983).
[17] Yu.M. Ostanevich, Time-of-flight small-angle scattering spectrometers on pulsed neutron sources, Macromol. Chem. Macromol. Symp. 15 (1988) 91–103.
[18] J.M. Holopainen, J. Lemmich, F. Richter, O.G. Mouritsen, G. Rapp, P.K.J. Kinnunen, Dimyristoylphosphatidylcholine/C16:0-ceramide binary liposomes studied by differential scanning calorimetry and wide- and small-angle X-ray scattering, Biophys. J. 78 (2000) 2459–2469.
[19] A. Bigi, N. Roveri, Fibre diffraction: collagen, in: S. Ebashi, M. Koch, E. Rubenstein (Eds.), Handbook on Synchrotron Radiation, 4, Elsevier Science Publishers B.V, Amsterdam, 1991, pp. 199–239.
[20] T.C. Huang, H. Toraya, T.N. Blanton, Y. Wu, X-Ray powder diffraction analysis of silver behenate, a possible low-angle diffraction standard, J. Appl. Crystallogr. 26 (1993) 180–184.
[21] C. Boulin, R. Kempf, M.H.J. Koch, S.M. McLaughlin, Data appraisal, evaluation and display for synchrotron radiation experiments: hardware and software, Nucl. Instrum. Meth. Phys. Res. Sect. A 249 (1986) 399–407.
[22] V. Luzzati, X-Ray diffraction studies of lipid–water systems, in: D. Chapman (Ed.), Biological Membranes, Academic Press, London, New York, 1968, pp. 71–124.
[23] J. Seddon, G. Cevc, Lipid polymorphism: structure and stability of lyotropic mesophases of phospholipids, in: G. Cevc (Ed.), Phospholipids Handbook, Marcel Dekker, Inc, New York, 1993, pp. 403–454.
[24] A. Tardieu, V. Luzzati, F.C. Reman, Structure and polymorphism of the hydrocarbon chains of lipids: a study of lecithin–water phases, J. Mol. Biol. 75 (1973) 711–733.
[25] S.T. Hyde, Identification of lyotropic liquid crystalline mesophases, in: K. Holmberg (Ed.), Handbook of Applied Surface and Colloid Chemistry, John Wiley and Sons, Ltd, London, 2001, pp. 299–332.
[26] J.N. Israelachvili, Intermolecular and Surface Forces, Academic Press, London, 1985.
[27] P.R. Cullis, B. de Kruijff, Lipid polymorphism and the functional roles of lipids in biological membranes, Biochim. Biophys. Acta 559 (1979) 399–420.
[28] S.M. Gruner, P.R. Cullis, M.J. Hope, C.P. Tilcock, Lipid polymorphism: the molecular basis of non-bilayer phases, Annu. Rev. Biophys. Biophys. Chem. 14 (1985) 211–238.
[29] K. Lohner, P. Balgavý, A. Hermetter, F. Paltauf, P. Laggner, Stabilization of non-bilayer structures by the etherlipid ethanolamine plasmalogen, Biochim. Biophys. Acta 1061 (1991) 132–140.
[30] P. Bednárová, Study of micellization and acid–base properties of tertiary amine local anesthetics, Magister Thesis, Faculty of Pharmacy, Comenius University, Bratislava, 1995.
[31] F. Andriamainty, J. Čižmárik, The critical micellar concentration of derivatives of piperidinoethylesters of 2-alkoxyphenylcarbamic acid, Pharmazie 58 (2003) 288.
[32] S.W. Hui, A. Sen, Effect of lipid packing on polymorphic phase behaviour and membranes properties, Proc. Natl. Acad. Sci. USA 86 (1989) 5825–5829.
[33] A.N. Goltsov, L.I. Barsukov, Synergetics of the membrane self-assembly: a micelle-to-vesicle transition, J. Biol. Phys. 26 (2000) 27–41.
[34] D. Uhríková, V. Cherezov, S. Yaradaikin, P. Balgavý, Mathematical model of the cut-off effect in the homologous series of tertiary amine local anesthetics, Pharmazie 48 (1993) 446–450.

[35] M. Pešák, F. Kopecký, J. Čižmárik, A. Borovanský, Study of local anesthetics. Part 70. Some physicochemical properties of piperidinoethylesters of alkoxyphenylcarbamic acid, Pharmazie 35 (1980) 150–152.
[36] D. Uhríková, J. Čižmárik, P. Balgavý, Interaction of surfactants with model and biological membranes. XIX. Partition and ionization equilibria of the local anaesthetic [2-(ethyloxy)phenyl]-2-(1-piperidinyl)ethyl ester of carbamic acid in the system phospholipid liposomes–aqueous phase, Čes. Slov. Farm. 44 (1995) 142–145.
[37] H. Hauser, Phospholipid vesicles, in: G. Cevc (Ed.), Phospholipids Handbook, M. Dekker, New York, 1993, pp. 603–637.
[38] R. Winter, W.C. Pilgrim, A SANS study of high pressure phase transitions in model biomembranes, Ber. Bunsen. Phys. Chem. 93 (1989) 708–717.
[39] W. Knoll, J. Haas, H.B. Stuhrmann, H.H. Füldner, H. Vogel, E. Sackmann, Small-angle neutron scattering of aqueous dispersions of lipids and lipid mixtures, J. Appl. Crystallogr. 14 (1981) 191–202.
[40] M. Dubničková, M. Kiselev, S. Kutuzov, F. Devínsky, V. Gordeliy, P. Balgavý, Effect of *N*-lauryl-*N*,*N*-dimethylamine *N*-oxide on dimyristoylphosphatidylcholine bilayer thickness: a small-angle neutron scattering study, Gen. Physiol. Biophys. 16 (1997) 175–188.
[41] D. Uhríková, P. Balgavý, N. Kucerka, A. Islamov, V. Gordeliy, A. Kuklin, Small-angle neutron scattering study of the *n*-decane effect on the bilayer thickness in extruded unilamellar dioleoylphosphatidylcholine liposomes, Biophys. Chem. 88 (2000) 165–170.
[42] D. Uhríková, N. Kučerka, A. Islamov, V. Gordeliy, P. Balgavý, Small-angle neutron scattering study of *N*-dodecyl-*N*,*N*-dimethylamine *N*-oxide induced solubilization of dioleoylphosphatidylcholine bilayers in liposomes, Gen. Physiol. Biophys. 20 (2001) 183–189.
[43] V.I. Gordelii, L.V. Golubchikova, A. Kuklin, A.G. Syrykh, A. Watts, The study of single biological and model membranes via small-angle neutron scattering, Progr. Colloid Polym. Sci. 93 (1993) 252–257.
[44] P. Balgavý, M. Dubničková, D. Uhríková, S. Yaradaikin, M. Kiselev, V. Gordeliy, Bilayer thickness in unilamellar extruded egg yolk phosphatidylcholine liposomes: a small-angle neutron scattering study, Acta Phys. Slov. 48 (1998) 509–533.
[45] P. Balgavý, N. Kučerka, V.I. Gordeliy, V.G. Cherezov, Evaluation of small-angle neutron scattering curves of unilamellar phosphatidylcholine liposomes using a multishell model of bilayer neutron scattering length density, Acta Phys. Slov. 51 (2001) 53–68.
[46] P. Balgavý, M. Dubničková, N. Kučerka, M.A. Kiselev, Bilayer thickness and lipid interface area in unilamellar extruded 1,2-diacylphosphatidylcholine liposomes: A small-angle neutron scattering study, Biochim. Biophys. Acta 1512 (2001) 40–52.
[47] F. Andriamainty, J. Čižmárik, D. Uhríková, P. Balgavý, Phospholipid liposomes-aqueous partition coefficients of alkyloxy homologs of local anesthetic heptacaine estimated by a surfactant ion sensitive electrode, in: E. Kukurová (Ed.), Advances in Medical Physics, Biophysics and Biomaterials, Malé Centrum, Bratislava, 1997, pp. 32–35.
[48] H. Hauser, L. Irons, The effect of ultrasonication on the chemical and physical properties of aqueous egg yolk lecithin dispersions, H.-S. Z. Physiol Chem. 353 (1972) 1579–1590.
[49] M. Bánó, P. Balgavý, Determination of the molar volume of the local anesthetic heptacaine and its propyloxy homologue in aqueous solution by means of a densitometer, Pharmazie 51 (1996) 512–513.
[50] M. Bánó, O. Pajdalová, Interaction of the local anaesthetic heptacaine with dipalmitoylphosphatidylcholine liposomes: a densimetric study, Biophys. Chem. 80 (1999) 53–66.
[51] R.C. Weast, Handbook of Chemistry and Physics, The Chemical Rubber Co, Cleveland, 1969.
[52] J. Národa, P. Balgavý, K. Gawrisch, J. Čižmárik, Effect of the local anesthetic heptacaine hydrochloride on the structured water in model phosphatidylcholine membrane: $^{2}$D-NMR and $^{31}$P-NMR study, Gen. Physiol. Biophys. 2 (1983) 457–471.
[53] K. Gawrisch, W. Richter, A. Möpps, P. Balgavý, K. Arnold, G. Klose, The influence of water concentration on the structure of egg yolk phospholipid/water dispersions, Stud. Biophys. 108 (1985) 5–16.
[54] B. Bechinger, J. Seelig, Conformational changes of the phosphatidylcholine headgroup due to membrane dehydration. A $^{2}$H-NMR study, Chem. Phys. Lipids 58 (1991) 1–5.
[55] D. Uhríková, Structural changes of lipid bilayers—effects of hydration, temperature and amphiphilic impurities, Ph.D. Thesis, Faculty of Mathematics and Physics, Comenius University, Bratislava, 1993.
[56] H.D. Dörfler, G. Brezesinski, H. Jantschke, Calorimetric studies of the thermodynamic properties of lamellar lecithin–local anesthetic–water mixtures, Liq. Cryst. 8 (1990) 263–277.
[57] P.R. Cullis, A.J. Verkleij, P.H. Ververgaert, Polymorphic phase behaviour of cardiolipin as detected by $^{31}$P NMR and freeze-fracture techniques. Effects of calcium, dibucaine and chlorpromazine, Biochim. Biophys. Acta 513 (1978) 11–20.
[58] A. Christiansson, H. Gutman, A. Wieslander, G. Lindblom, Effects of anesthetics on water permeability and lipid metabolism in *Acholeplasma laidlawii* membranes, Biochim. Biophys. Acta 645 (1981) 24–32.
[59] D.N. Brindley, M. Bowley, Drugs affecting the synthesis of glycerides and phospholipids in rat liver. The effects of clofibrate, halofenate, fenfluramine, amphetamine, cinchocaine, chlorpromazine, demethylimipramine, mepyramine and some of their derivatives, Biochem. J. 148 (1975) 461–469.
[60] L. Horáková, S. Štolc, Comparison of the effects of carbisocaine and other local anesthetics on $^{32}$P incor-

poration into individual and total phospholipids in synaptosomes, Gen. Physiol. Biophys. 7 (1988) 81–93.

[61] E. Garcia-Martin, C. Gutierrez-Merino, Local anesthetics inhibit the $Ca^{2+}$, $Mg^{2+}$-ATPase activity of rat brain synaptosomes, J. Neurochem. 47 (1986) 668–672.

[62] E. Garcia-Martin, C. Gutierrez-Merino, Modulation of the $Ca^{2+}$, $Mg^{2+}$-ATPase activity of synaptosomal plasma membrane by the local anesthetics dibucaine and lidocaine, J. Neurochem. 54 (1990) 1238–1246.

[63] C. Gutierrez-Merino, A. Molina, B. Escudero, A. Diez, J. Laynez, Interaction of the local anesthetics dibucaine and tetracaine with sarcoplasmic reticulum membranes. Differential scanning calorimetry and fluorescence studies, Biochemistry 28 (1989) 3398–3406.

[64] F. Andriamainty, J. Filípek, P. Kovács, P. Balgavý, Effect of local anesthetic [2-(alkyloxy)phenyl]-2-(1-piperidinyl)ethyl esters of carbamic acid on the activity of purified sarcoplasmic reticulum (Ca–Mg)ATPase, Pharmazie 51 (1996) 242–245.

[65] G.A. Senisterra, J.R. Lepock, Thermal destabilization of transmembrane proteins by local anaesthetics, Int. J. Hyperther. 16 (2000) 1–17.

[66] A.G. Lee, How lipids interact with an intrinsic membrane protein: the case of the calcium pump, Biochim. Biophys. Acta 1376 (1998) 381–390.